SAND2007-4222C

A Three-Component Balance System for Measuring Forces and Moments in Fin-Wake Interactions

Justin A. Smith,[1] John F. Henfling,[2] Steven J. Beresh,[3] Thomas W. Grasser,[4] and Russell W. Spillers[5]
Sandia National Laboratories[6], P. O. Box 5800 Albuquerque, NM 87185

Maneuvering atmospheric flight vehicles often combine tail fins and upstream fins or canards for stability and control. As an upstream fin is pitched to angle of attack, a large pressure differential produces a vortex that rolls off of the leading edge of the fin and travels downstream towards the tail of the vehicle. This shed vortex may interact with a tail fin and alter its aerodynamic characteristics in unusual ways, making the prediction of forces on the fin, and hence the control of the vehicle, extremely difficult. In this study, a three-component balance system has been developed and implemented to measure the forces and moments on a sub-scale model of a missile fin in the presence of the wake and shed vortex from an upstream fin. Measurements were made from Mach 0.5 – 0.8 with both the upstream and downstream fins pitched between -5° and 10° angle of attack. Results show an induced angle of attack on the downstream fin that grows as the upstream fin's shed vortex grows stronger as its angle of attack is increased. The influence of Mach Number was found to grow stronger as the angles of attack of the upstream and downstream fins diverged.

1. Introduction

Maneuvering atmospheric flight vehicles often combine tail fins with upstream fins or canards for stability and control. In such vehicles, an interaction may be seen between the vortex shed by an upstream fin and a tail fin, which, if careful attention is not made to accurately measure or predict the resulting forces at every possible combination of flowfield and relative fin positions, may alter the forces and moments on the tail fin in unpredictable ways. Modern design and development of flight vehicles depends on correlation-based tools and CFD, which must be able to accurately predict complicated flowfields such as those encountered when the vortex of an upstream fin or canard impinges on a tail fin. These tools rely on wind tunnel and flight tests for validation of the mathematical models they incorporate to simulate such flows. A comprehensive experimental study of this interaction spanning the range of flight conditions that the vehicle may encounter is thus needed for a full code certification.[1,2]

Previous studies have focused primarily on measuring the forces and moments on an entire finned vehicle configuration without regard to the component loading on the fins.[3-5] Although some studies have been done on instrumented fins[6] and slender body theory has been applied in many cases for fin load estimation,[7-9] there is little mention of the downstream influence from the wake of an upstream fin, and those reports that do discuss such an interaction are typically done on double delta wings with a fixed separation between the leading and trailing fin.[10-14] While these reports do provide valuable information on the vortex-fin interaction, more useful information for CFD code certification, and an improved understanding of the underlying physics, is gained through a comprehensive wind tunnel study on a representative sub-scale model.

[1] Aerosciences Department, MS 0825, Engineering Sciences Center, E-mail: jussmit@sandia.gov. Member, AIAA.
[2] Aerosciences Department, MS 0825, Engineering Sciences Center, E-mail: jfhenfl@sandia.gov. Member AIAA.
[3] Aerosciences Department, MS 0825, Engineering Sciences Center, E-mail: sjberes@sandia.gov. Senior Member AIAA.
[4] Thermal/Fluid Experimental Sciences, MS 0834, Engineering Sciences Center, E-mail: twgrass@sandia.gov.
[5] Aerosciences Department, MS 0825, Engineering Sciences Center, E-mail: rwspille@sandia.gov.

Sandia is a multiprogram laboratory operated by Sandia Corporation, a Lockheed-Martin Company, for the United States Department of Energy's National Nuclear Security Administration under Contract DE-AC04-94AL85000.

For this study, a three component fin balance system has been designed and utilized to measure the forces and moments on several fin geometries on a flat plate from Mach 0.5 to 0.8 in order to provide data for CFD code validation, provide a database to aid in future vehicle design, and to identify interesting cases to be studied using Particle Image Velocimetry (PIV), Pressure Sensitive Paint (PSP), and possibly other flow visualization and measurement techniques. Force measurements were taken for several combinations of flow conditions, fin geometries, and angles of attack between -5° and 10° in nominally 1° increments. This paper describes the balance system, experimental setup, and force measurement results on single fins and in an interaction between the shed vortex and wake of an upstream and a downstream fin from Machs 0.5 to 0.8. Investigations for transonic flow up to Mach 1.2 are currently under way and will be documented in a later paper.

2. Experimental Apparatus

Trisonic Wind Tunnel

Experiments were performed in Sandia's Trisonic Wind Tunnel (TWT), which is a blowdown-to-atmosphere facility using air as the test gas through a 305 x 305 mm^2 (12 x 12 $inch^2$) rectangular test section enclosed within a pressurized plenum. A solid-wall transonic test section was used rather than the traditional ventilated version because it offers reasonable optical access, a flat plate on which the fins reside, and computationally tractable boundary conditions for comparison of experimental data and numerical simulations. The use of a solid-wall test section limits the Mach Number range of the flowfield, but this was not an issue for the conditions explored thus far. Future tests at transonic Mach Numbers will be performed with using a half-body configuration with porous plates on three of the tunnel walls to alleviate transonic choking.

Fin Hardware

A variety of fin geometries are used on existing vehicles, all of which could not be studied in this analysis. Thus, a generic fin shape was chosen to represent the multiple real-world geometries. Five variations of the baseline geometry were selected for the current analysis, all having trapezoidal planform with 45° leading edge sweep, no trailing edge sweep, and aspect ratio of 2/3. All fins have sharp leading edges which constantly expand toward the trailing edge until a uniform thickness is reached at a distance, x, from the leading edge. On four of the fins, x varies linearly over the fin's span from root to tip so as to maintain a constant ratio of 1/3 of the local chord. For the fifth fin, a constant x of 25.4 mm (1 inch) was used. The baseline fin, Fin A, has a thickness of 3.175 mm (0.125 inches), root chord of 76.2 mm (3 inches), a span of 38.1 mm (1.5 inches), and tip chord of 38.1 mm (1.5 inches). Fin B is a 6.35 mm (0.25 inch) thick version of Fin A, and Fin C is also identical to Fin A except with a constant x of 25.4 mm (1 inch). Fins D and E are just scaled up versions of Fin A with root chords of 101.6 and 152.4 mm (4 and 6 inches), respectively. All fins are composed of stainless steel with a black oxide coating to allow for additional testing with PIV. Figure 1 displays the shape and geometric parameters of the five fins. The fin geometry parameters are displayed in Table 1. Planform areas, S, and bending and hinge moment reference lengths (l_b and l_h) are also given.

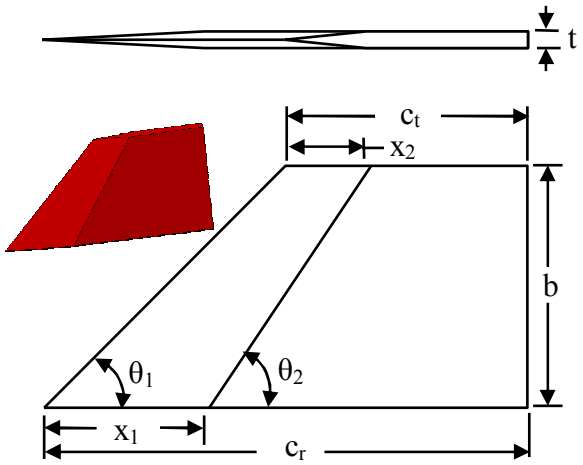

Figure 1. Fin geometric parameters.

Table 1. Fin Geometric Parameters. Lengths are in mm, areas in mm^2, and angles in degrees.

Fin	t	c_r	b	θ_1	x_1	θ_2	c_t	x_2	S	l_b	l_h
A	3.2	76.2	38.1	45.0	25.4	56.3	38.1	12.7	2117.4	38.1	57.2
B	6.4	76.2	38.1	45.0	25.4	56.3	38.1	12.7	2117.4	38.1	57.2
C	3.2	76.2	38.1	45.0	25.4	45.0	38.1	25.4	2117.4	38.1	57.2
D	3.2	101.6	50.8	45.0	33.8	56.3	50.8	16.9	3871.0	50.8	76.2
E	3.2	152.4	76.2	45.0	50.8	56.3	76.2	25.4	8709.7	76.2	114.3

Fin Force Balance and Attachment Hardware

A fin is attached to one of two three-component (normal force, bending moment, and hinge moment) force balances supplied by *Allied Aerospace's Force Measurement Systems Division*. Fins are attached to the balance through one of the solid walls of the test section via a cylindrical adaptor hub such that the fin resides within the test section, at a 0.06 inch gap from to the wall, and the balance sets on the outside of the test section. The cylindrical hub allows for the angle of attack of the fin to be changed by rotating the fin along with the entire balance system. Since the fin and balance are rotated together, the measured force components are always in the local fin body coordinate system, and no coordinate system transformation is needed. Additionally, this allows for the fin angle of attack setting mechanism to be located at the top of the balance canister and out of the tunnel. The system allows for very precise and repeatable angle settings from -5° to 10° in 1° increments. A photograph of the fin balance in the TWT with an attached fin, and a diagram insert to show the connection of fin to balance through the tunnel wall, is provided in Figure 2. In this photo, the flow path is from right to left.

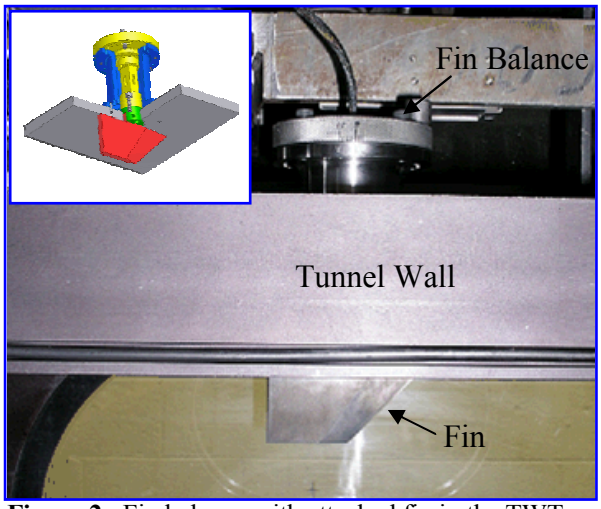

Figure 2. Fin balance with attached fin in the TWT.

The fin axial position is set with sliding inserts on the tunnel top wall. This allows the whole system, balance and all, to be adjusted upstream or downstream as needed for two-fin studies. The inserts were composed of aluminum and covered with a black anodized coating. For all of the measurements presented in this analysis, the instrumented fin was located 508 mm (20 inches) downstream of the contraction, i.e. 508 mm from the beginning of the test section. Thus, the fin always saw the same boundary layer.

The balance system is capable of acquiring data for normal force, root bending moment, and hinge moment, with maximum loads of 222 N, 7.0 N-m, and 2.9 N-m (50 lbs., 62 in-lbs., and 26 in-lbs), respectively, for the three components. A larger balance capable of 890 N, 28.2 N-m, and 12.7 N-m (200 lbs., 250 in-lbs., and 112 in-lbs.) was also acquired and will be used for later tests at transonic speeds up to Mach 1.2. These balance load ranges were sized using an Air Force correlation-based missile design code, Missile Datcom,[15] and an Euler CFD code, Splitflow,[16] for single and aligned fins at the test freestream conditions. For the smaller balance, the manufacturer's quoted calibration uncertainty, calculated as the 95% confidence levels from the manufacturer calibration's standard deviations, were 0.14% full-scale normal force, 0.23% full-scale bending moment, and 0.12% full-scale for the hinge moment. Check loads were applied to the smaller fin balance once it arrived from the manufacturer, and it was determined that the manufacturer's calibration data was accurate, but since differences existed in the data reduction methods of the fin balance manufacturer and Sandia, the manufacturer's data was re-reduced to yield a more accurate calibration matrix for use with Sandia's data reduction programs.

Forces and moments were measured in coefficient form, normalized by the local dynamic pressure, q, fin planform area, S, and bending moment and hinge moment reference lengths, l_b and l_h. The normal force coefficient, C_{NF} = NF/qS, was defined to be positive into the page when acting on a fin oriented as in Figure 2. The bending moment coefficient, C_{BM} = BM/qSl_b, is referenced about the tunnel wall and a positive moment would tend to roll the fin's tip into the page. The hinge moment coefficient, C_{HM} = HM/qSl_h, is referenced about the fin's root half-chord, and positive moment would roll the fin's leading edge into the page and its trailing edge out of the page.

Experimental Conditions

Instrumented fins were tested at freestream Mach Numbers, set at the beginning of the test section 508 mm upstream of the fin, of $M_{\infty,1}$ = 0.5, 0.6, 0.7, and 0.8. Because of boundary layer growth and tunnel blockage, the local fin Mach numbers, $M_{\infty,2}$, were nominally 0.52, 0.61, 0.72, and 0.84, depending on fin size and angle of attack. The wind tunnel stagnation pressures were P_0 = 121 kPa (17.6 psia) for $M_{\infty,1}$ = 0.5, 130 kPa (18.9 psia) for $M_{\infty,1}$ = 0.6, 142 kPa (20.6 psia) for $M_{\infty,1}$ = 0.7, and 156 kPa (22.6 psia) for $M_{\infty,1}$ = 0.8, which yields a freestream static pressure of P = 102 kPa (14.8 psia) for all cases. The nominal tunnel stagnation temperature was T_0 = 325 K (585 °R). Under these conditions, freestream unit Reynolds numbers were 11×10^6 m^{-1} at $M_{\infty,1}$ = 0.5, 13×10^6 m^{-1} at $M_{\infty,1}$ = 0.6, 16×10^6 m^{-1} at $M_{\infty,1}$ = 0.7, and 22×10^6 m^{-1} at $M_{\infty,1}$ = 0.8. The tunnel conditions for all cases are

Table 2. Experimental Conditions.

$M_{\infty,1}$	$M_{\infty,2}$	P_0, kPa	P, kPa	T_0, K	RE, m^{-1}
0.5	0.52	121	102	325	11×10^6
0.6	0.61	130	102	325	13×10^6
0.7	0.72	142	102	325	16×10^6
0.8	0.84	156	102	325	22×10^6

summarized in Table 2.

Boundary layer profiles and other tunnel properties have been examined and reported for the TWT by Beresh et.al.[17] In that paper, the boundary layer thickness was found to range from 14.5 mm (0.57 inches) at Mach 0.5 to 13.5 mm (0.53 inches) at Mach 0.8 under tunnel operating conditions similar to those used in this analysis.

3. Uncertainty Analysis

Data uncertainties (U) exist in this system as both systematic, or bias errors (B); and random, or precision errors (P). Possible sources of error include, but are not limited to, flow condition bias and repeatability, strain gage temperature and electronics effects, and hardware related errors such as fin angle and location setting bias and repeatability. Care has been taken to eliminate the bias errors as much as possible, for example, the strain gage readings were temperature compensated and fin angles were set with a tightly toleranced pin to provide accurate and repeatable angle settings. However, bias errors still exist because measurements were made on a single wall of a single wind tunnel with its own unique flowfield, and to eliminate all of these bias errors would require a much broader and more time intensive test, which is not in the scope of this work. So, care must be taken to recognize that the results in this report are applicable to the specific test conditions used in this analysis only, and that any comparison for CFD validation purposes should be made at identical conditions to this test.

With that said, the measurement uncertainty consists of the remaining precision errors, all of which are accounted for if enough repeat runs are taken spread throughout the test. Six runs at each Mach Number for the specific cases of a single baseline fin at 5° angle of attack, and for two fins separated by 4 fin lengths, with $\alpha_1 = 10°$ and $\alpha_2 = 0°$, were performed. The repeat runs gave a consistent measurement of uncertainty in the final engineering quantities, U_{CNF}, U_{CBM}, and U_{CHM}, of about 0.2% of the balance full-scale.

4. Results

Reynolds Number Effect

The effect of Reynolds Number on the force coefficients was investigated for the baseline fin at Mach 0.8 and 5^o angle of attack. Three Reynolds Numbers covering the range of the TWT's possible operating conditions, from 12×10^6 m^{-1} to 23×10^6 m^{-1}, were chosen for analysis. Additionally, two-fin data were obtained at several Reynolds Numbers to ascertain whether there is an effect on the vortex shed from an upstream fin sufficient enough to measurably affect the downstream fin's forces. The results of this analysis were that the normal force and bending moment coefficients were not significantly affected, while the hinge moment coefficient increased with Reynolds Number. The cause of this change with Reynolds Number is still under investigation, thus, the results discussed herein are biased to the Reynolds Numbers of this analysis. As a result, Reynolds Number should be matched to these tunnel conditions as closely as possible when making comparisons to other data or for code validation in order to eliminate the differences due to Reynolds Number.

Single Fin Results

The coefficients of normal force, bending moment, and hinge moment for the baseline fin (Fin A) are displayed for Machs 0.5 to 0.8 in Figures 3 through 5. For all three components, to within the measurement uncertainty, the data are symmetric about zero angle of attack, suggesting that any tunnel flow angularity does not have a noticeable effect on the measurements. Above 5° angle of attack, the normal force and pitching moment coefficients experience a slope increase due to vortex lift, a suction force on the fin body induced by the vortex generated at the fin's leading edge. This effect is increased as stronger vortices are generated with increasing angle of attack and Mach Number. Figures 3 and 5 suggest that at high angles of attack and higher Mach Numbers there is a competing effect of increased normal force and of the center of pressure being pushed back towards the center of the fin, resulting in a reduction in the slope of C_{HM}. Future tests with PIV, PSP, and possibly oil flow visualization in the region of the leading edge, will help to better determine the mechanism of the slope changes above 5° angle of attack.

Figures 6 through 8 compare the normal force, bending moment, and hinge moment coefficients at Mach 0.8 for all five of the fins. The differences in the force coefficients between different fins are of the same order of magnitude as the difference seen in the single fin data at different Mach Numbers. A trend is seen in the normal

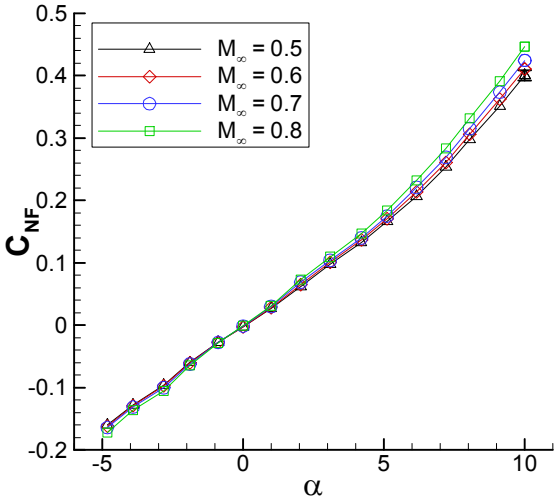

Figure 4. Normal force coefficient for the baseline fin.

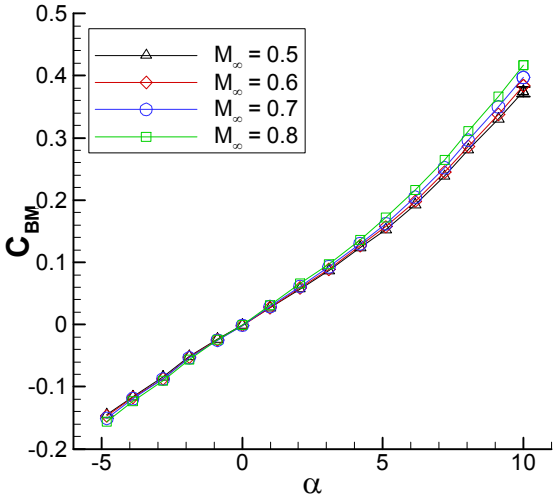

Figure 5. Bending moment coefficient.

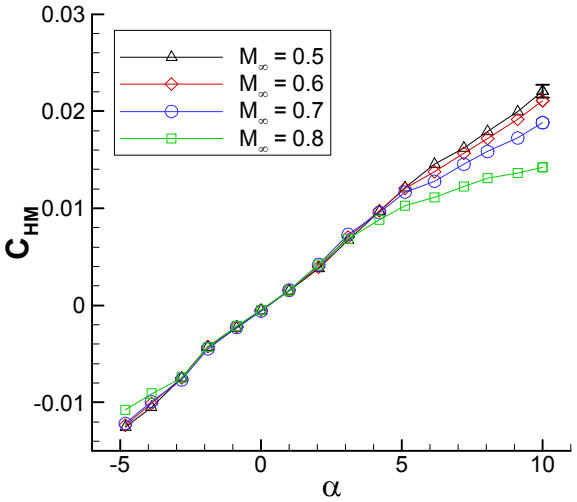

Figure 6. Hinge moment coefficient.

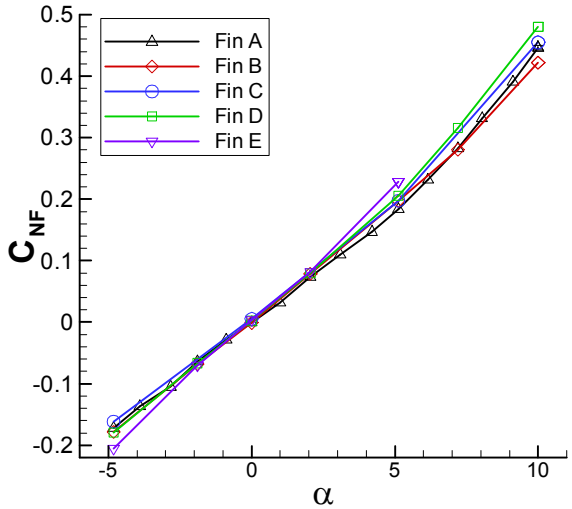

Figure 7. Normal force coefficients for all single fin configurations at Mach 0.8.

force and hinge moment coefficient data, Figures 7 and 8, in which the slopes are greater for the larger two fins (Fins D and E) than for the smaller fins. A likely cause for the greater slopes in C_{NF} and C_{HM} for the larger fins is that there is less of an interaction of those fins' vortices with the tunnel wall boundary layer, which is over a third of the span of the smaller fins but only 27% of the span of Fin D and 18% of the span of Fin E. A vortex at the tip of a fin thus has a greater chance to interact with the boundary layer for the smaller fins. Compressibility effects may also be a factor, as the larger fins cause more tunnel blockage, and thus a greater local Mach number, especially as they are set to high angles of attack. The mechanism for these differences is certainly not solved in this analysis and warrant further investigation. PIV and PSP should provide a perfect means to establish the mechanism involved in this interaction.

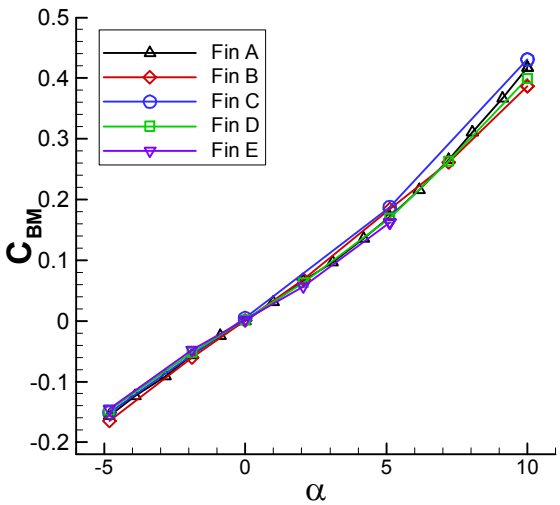

Figure 8. Bending moment coefficients.

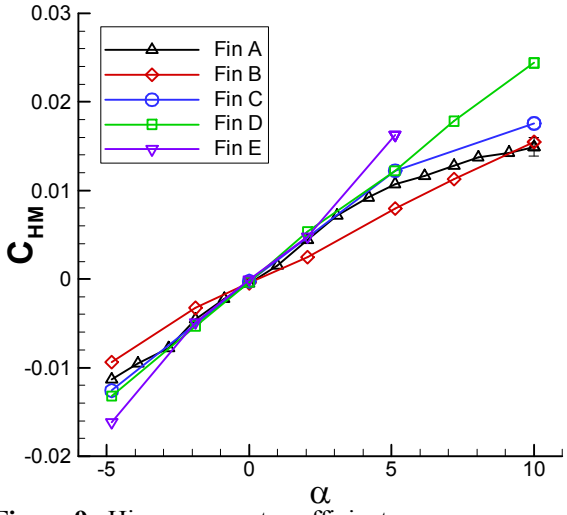

Figure 9. Hinge moment coefficients.

Two-fin data are presented in Figures 9 through 11 for the case of the baseline fin at a distance of 4 fin lengths (304.8 mm) downstream of another baseline fin, measured from fin center to fin center. In these figures, the downstream fin's forces are plotted as a function of its angle of attack, α_2, with different curves drawn for each upstream fin angle of attack, α_1, and Mach Number. For comparison, the single fin data are shown with symbols. The primary influence of the upstream fin is to shift the downstream fin's forces downward for positive upstream fin angle of attack, and upward for negative upstream fin angle of attack. This shift is caused by an interaction where the upstream fin's shed tip vortex induces an angle of attack on the downstream fin. The influence of Mach Number on the measured forces grows stronger as the angles of attack of the upstream and downstream fins diverge. This effect is likely due to the position of the downstream fin's leading edge relative to the position of the upstream shed vortex. Similar behavior is seen in the bending moment coefficient, but the hinge moment coefficient magnitude decreases slightly with Mach Number. The effect of this aerodynamic interaction between an upstream shed vortex and a downstream fin is currently under investigation and will be reported at the 22nd International Congress on Instrumentation in Aerospace Simulation Facilities in Reference [18].

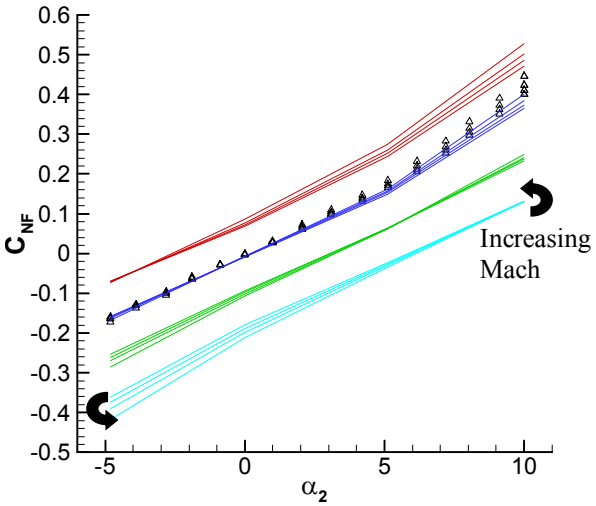

Figure 10. Normal force coefficients of Fin A at 4 fin lengths downstream of Fin A.

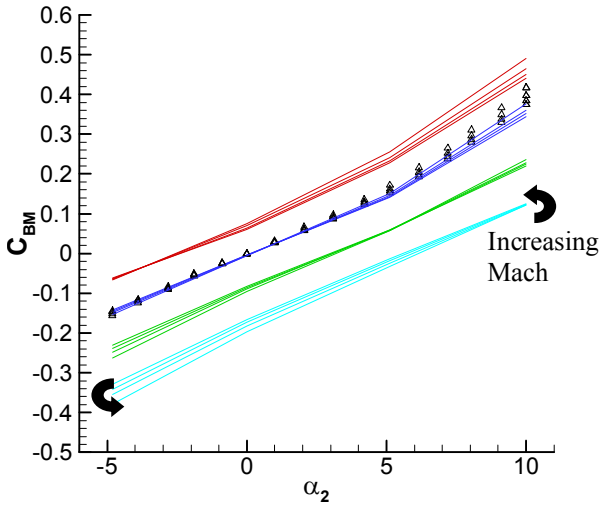

Figure 11. Bending moment coefficients.

5. Conclusions and Future Work

Maneuvering atmospheric flight vehicles often combine tail fins and upstream fins or canards for stability and control. As an upstream fin is pitched to angle of attack, a large pressure differential produces a vortex that rolls off of the leading edge of the fin and travels downstream towards the tail of the vehicle. This shed vortex may interact with a tail fin and alter its aerodynamic characteristics in unusual ways, making the prediction of forces on the fin, and hence the control of the vehicle, extremely difficult. To study this effect, a sub-scale experiment was designed to measure the forces and moments of a fin in the presence of the vortex shed by an upstream fin. Measurements were made with fins mounted on one wall of Sandia's Trisonic Wind Tunnel (TWT) with subsonic flow from Mach 0.5 to 0.8 and both the upstream and downstream fins pitched between -5° and 10° angle of attack. Effects of Reynolds Number, Mach Number, fin geometry, and angle of attack were studied and reported in this analysis.

Single fin results showed that vortex lift caused a slope increase in normal force and bending moment

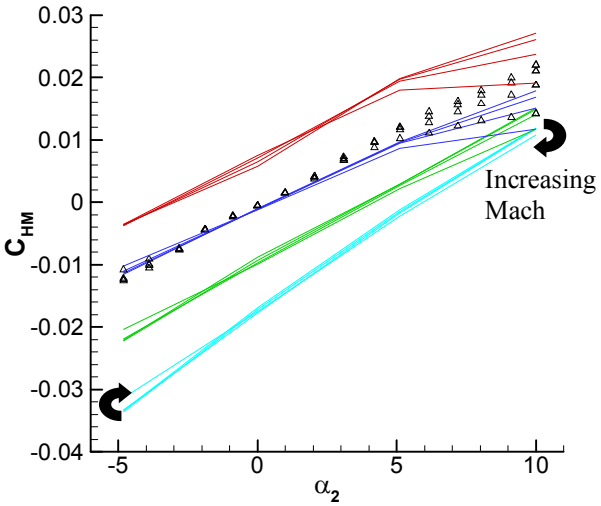

Figure 12. Hinge moment coefficients.

above 5° angle of attack. The hinge moment coefficient slope actually decreases at higher angle of attack, suggesting that the center of pressure is being pushed back toward the center of the fin. Mach Number was seen to enhance these trends as stronger vortices and greater compressibility were generated.

A comparison of several fin geometries for the single fin case showed an increased slope in C_{NF} and C_{HM} for the larger fins, and little change from the baseline fin's values for the thicker and differently tapered fins. This suggests that differences in the interaction between the fins' vortices and the tunnel wall boundary layer for different sized-fins were the cause of the force and moment discrepancy.

Finally, two-fin data results were presented for the case of two baseline fins separated axially by four fin lengths. Results show that the upstream shed vortex induces an angle of attack on the downstream fin that grows as the upstream fin's shed vortex grows stronger as its angle of attack is increased. The influence of Mach Number was found to grow stronger as the angles of attack of the upstream and downstream fins diverged, likely because of the relative position of the downstream fin's leading edge to the shed vortex.

Work is currently being conducted to ascertain the behavior of the fin-wake interaction at transonic speeds up to Mach 1.2 for fins in a half-body configuration where three of the tunnel's four walls are porous. This study at higher Mach Numbers will examine the effects of transonic nonlinearities in the data, trying to see if the relatively well-behaved results up to Mach 0.8 grow more complicated near Mach 1. Additionally, Particle Image Velocimetry is being used to gain a better understanding of the wake flow created by an upstream fin and its interaction with a trailing fin. Finally, a Pressure Sensitive Paint calibration chamber and pressure tapped fin have been constructed and studies to determine the pressure and force distribution over the entire trailing fin using Pressure Sensitive Paint will begin shortly.

References

[1]Aeschliman, D. P. and Oberkampf, W. L., "Experimental Methodology for Computational Fluid Dynamics Code Validation," *AIAA Journal*, Vol. 36, No. 5, 1998, pp. 733-714.

[2]Oberkampf, W. L. and Blottner, F. G., "Issues in Computational Fluid Dynamics Code Verification and Validation," *AIAA Journal*, Vol. 36, No. 5, 1998, pp. 687-695.

[3]Despirito, J., Vaughn, M. E., and Washington, W. D., "CFD Investigation of Canard-Controlled Missile with Planar and Grid Fins in Supersonic Flow," AIAA Paper 2002-4509, Aug. 2002.

[4]Frantz, G. E., "Static Stability and Force Characteristics of a 0.02-Scale Model of the Saturn C-1 Launch Vehicle with Apollo Payload for Mach Number 0.31," North American Aviation, Inc., NAS9-150, Feb. 1963.

[5]Murman, S. M. and Aftosmis, M. J., "Cartesian-Grid Simulations of a Canard-Controlled Missile with a Spinning Tail," AIAA Paper 2003-3670, June 2003.

[6]Allen, C. Q., Schwind, R. G., and Malcolm, G. N., "Canard-Body-Tail Missile Test at Angles of Attack to 50° in the Ames 11-Foot Transonic Wind Tunnel," NASA-TM-78441, Sept. 1978.

[7]Hemsch, M. J., Nielsen, J. N., Smich, C. A., and Perkins, S. C., "Component Aerodynamic Characteristics of Banked Cruciform Missiles with Arbitrary Control Deflections," AIAA Paper 77-1153, Aug. 1977, pp. 288-299.

[8]Oberkampf, W. L., "Prediction of Forces and Moments on Finned Missiles in Subsonic Flow," AIAA Paper 79-0365, Jan. 1979.

[9]Oberkampf, W. L., "Prediction of Forces and Moments on Finned Bodies at High Angle of Attack in Transonic Flow," Sandia National Lab., SAND80-2380, Albuquerque, NM, April 1981.

[10]Fritzelas, A. E., Platzer, M. F., and Hebbar, S. K., "Effects of Reynolds Number of the High-Incidence Flow Over Double-Delta Wings," AIAA Paper 97-0046, Jan. 1997.

[11]Liu, P., Wen, R., and Zhang, G., "Effects of Canard Sweep and Canard-Spanwise Blowing Magnitude on Lift Increment," *Journal of Aircraft*, Vol. 43, No. 5, Sept. 2006, pp. 1369-1371.

[12]Bergmann, A. and Hummel, D., "Aerodynamic Effects of Canard Position on a Wing Body Configuration in Symmetrical Flow," AIAA Paper 2001-0116, Jan. 2001.

[13]Erickson, G. E., Schreiner, J. A., and Rogers, L. W., "On the Structure, Interaction, and Breakdown Characteristics of Slender Wing Vortices at Subsonic, Transonic, and Supersonic Speeds," AIAA Paper 89-3345, Aug. 1989.

[14]Ma, B., Liu, P., and Wei, Y., "Effects of Wing and Canard Sweep on Lift Enhancement of Canard Configurations," *Journal of Aircraft*, Vol. 41, No. 6, Nov. 2004, pp. 1521-1523.

[15]Blake, W. B., "Missile DATCOM: User's Manual – 1997 Fortran 90 Revision," U.S. Air Force Research Lab/Air Vehicles Directorate, Wright-Patterson Air Force Base, OH, 1998.

[16]Karman, S. L., "SPLITFLOW: A 3D Unstructured Cartesian/Prismatic Grid CFD Code for Complex Geometries," AIAA-95-03436.

[17]Beresh, S. J., Henfling, J. F., Spillers, R. W., and Erven, R. J., "Measurement of Experimental Boundary Conditions for CFD Validation of a Supersonic Jet in Transonic Crossflow," AIAA Paper 2006-3449, June 2006.

[18] Beresh, S. J., Smith, J. A., Henfling, J. F., Grasser, T. W., and Spillers, R. W., "A Combined PIV / Force Balance Study of a Fin-Wake Aerodynamic Interaction," Submitted to the 22nd International Congress on Instrumentation in Aerospace Simulation Facilities, Pacific Grove, CA, 10-14 June, 2007.